AN EXPERIMENTAL STUDY ON DAMAGE AND REPAIR EFFECTIVENESS OF REINFORCED CONCRETE COLUMNS SUBJECTED TO REVERSE CYCLIC LOADING WITH LARGE DEFORMATION

(Translation from Proceedings of JSCE, No.648/V-47, May 2000)




Tadayoshi ISHIBASHI Takeshi TSUYOSHI Kaoru KOBAYASHI Masashi KOBAYASHI

Rational seismic design demands precise estimates of damage levels to RC columns in the large plastic deformation range. We carry out reversed cyclic loading tests on RC model columns with large deformation capacities, and estimate damage levels corresponding to degrees of plastic deformation in consideration of ease of repair. Furthermore, ranges of serious damage are examined. We also perform reverse cyclic loading tests on repaired RC model columns, thereby confirming the effectiveness of repairs. From these experiments and related considerations, damage levels for seismic resistant design and the effectiveness of repairs in the large plastic deformation range are made clear.

Keywords: *seismic resistant design, reversal cyclic loading, reinforced concrete column, damage, repair*

Tadayoshi Ishibashi is a manager in the Structural Engineering Center of the Construction Department of East Japan Railway Company. He obtained his D.Eng from the University of Tokyo in 1983. His research interests relate to the seismic design of concrete structures for railways. He is a fellow member of the JSCE.

Takeshi Tsuyoshi is a group leader in the Tokaido Sobu Department at the Tokyo Construction Office of East Japan Railway Company. He obtained his D.Eng from the University of Tokyo in 2001. His research interests relate to the seismic design of concrete structures for railways. He is a member of the JSCE.

Kaoru Kobayashi is a group leader in the Research & Development Center of East Japan Railway Company. He obtained his D.Eng from the University of Tokyo in 2001. His research interests relate to the seismic design of concrete structures for railways. He is a member of the JSCE.

Masashi Kobayashi is a member in the Structural Engineering Center of the Construction Department of East Japan Railway Company. His research interests relate to the seismic design of concrete structures for railways. He is a member of the JSCE.

1. INTRODUCTION

Ductility design has conventionally formed the basis of seismic resistant design for concrete railway structures[1], with plastic deformation capacity determining the ability of a structure to absorb earthquake energy and an acceptable degree of damage or plasticization being set in consideration of its behavior beyond the plastic point. However, since earthquake resistance is defined in terms of ease of recovery for structures with varying degrees of importance[2][3], there is a need to control the level of damage sustained by structural members, as this affects the ease of repair. For rational seismic design, therefore, there is a need to correctly assess the correlation between damage and degree of plastic deformation of structures (members) in an earthquake.

To evaluate the correlation between damage and deformation levels and to investigate damage range, we performed static reverse cyclic loading tests on RC specimens with a large deformation capacity (with a ductility factor of 10 or more) modeling a rigid-frame railway viaduct column[4].

This paper discusses the effects of various factors on the damage caused and the relationship between damage and plastic deformation, which is closely related to the ease of repair. We then applied several methods of repair to RC specimens damaged in the plastic deformation range and subjected them to further reverse cyclic loading tests. The deformation capacity and repair effectiveness after reverse cyclic loading are also discussed[5].

2. OUTLINE OF TESTS

2.1 Specimen dimensions

Table 1 and **Figure 1** show the dimensions and cross sections of the various specimens, respectively. The specimens are 1/2-scale models of actual rigid-frame railway viaduct columns. The major test parameters were:

* Sectional form
* Shear span ratio (a/d)
* Axial reinforcement ratio ($pa := \Sigma As/(B \cdot D)$

  where,

  ΣAs: Total sectional area of axial reinforcement

  B: Width of column section

  D: Height of column section
* Hoop reinforcement ratio (ps)
* Axial compressive stress density (σ'no)

The parameter ranges adopted in the tests were:

* Axial reinforcement ratio (pa): 0.63 to 4.42%
* Hoop reinforcement ratio (ps): 0.45 to 2.27%
* Axial compressive stress density (σ'no): 0.49 to 4.9 centering on 0.98 (N/mm^2)

Table 2 shows the material strengths and calculated strength ratio (Vyd/Vmu)

Where,

Vyd: Shear strength of members

Vmu: = Mu/la

Mu: Bending strength

la: Shear span

We used the actual material strengths determined by material tests in Table to calculate the strength ratio [1], with shear strength (Vcd) calculated according to the formula by Niwa et al. (for a/d>=2.5) and that by Ishibashi et al. (for 2.5>=a/d>=0.5)[6][7] on the assumption that the partial safety factor has a value of 1.0. The strength ratio of the specimens used in this study was in the range 1.55 to 4.18.

Table 1 Dimensions of specimens

Specimen No.	Size of section B x H (mm)	Effective height d (mm)	Shear span ratio a / d	Axial rein-forcement (diameterxquantity)	Axial reinforce-ment ratio pa=As / (Bxd) (%)	Side rein-forcement (diameterxquantity)	Hoop rein-forcement (dia) - (set) (interval) (interval: mm)	Hoop reinforce-ment ratio ps (%)	Axial compressive stress intensity σ'no (N/mm^2)	Loading pattern
I - 1	400x400	360	3.19	D19x16	2.865	D19x3	D13-1ctc125	0.507	0.98	A
I - 2	400x400	360	3.19	D19x16	2.865	D19x3	D13-1ctc 70	0.905	0.98	A
I - 3	400x400	360	3.19	D19x16	2.865	D19x3	D13-1ctc 40	1.584	0.98	A
II- 1	400x400	360	3.19	D16x16	1.986	D16x3	D13-1ctc 90	0.704	0.49	A
II - 2	400x400	360	3.19	D16x16	1.986	D16x3	D13-1ctc 50	1.267	1.96	A
III - 1	400x600	550	2.09	D13x12	0.634	D13x2	D13-1ctc 90	0.704	0.98	A
III - 2	400x350	300	4.17	D22x16	4.424	D22x3	D13-1ctc 90	0.704	0.98	A
III - 3	350x350	310	3.83	D19x16	3.742	D19x3	D16-1ctc 50	2.270	4.90	A
A 1	400x400	360	3.19	D19x16	2.865	D19x3	D13-1ctc 80	0.792	0.98	B
A 2	400x400	360	3.19	D19x16	2.865	D19x3	D13-1ctc 60	1.056	0.98	B
A 3	400x400	360	3.19	D16x16	1.986	D16x3	D13-1ctc 70	0.905	0.49	B
A 4	400x400	360	3.19	D13x16	1.267	D13x3	D13-1ctc 80	0.792	0.98	B
A 5	400x400	360	3.19	D13x16	1.267	D13x3	D13-1ctc140	0.453	0.98	B
A 6	400x400	360	3.19	D19x16	2.865	D19x3	D13-1ctc 50	1.267	0.98	B
A 7	400x400	360	3.19	D19x16	2.865	D19x3	D13-1ctc 60	1.056	0.98	A
A 8	400x400	360	3.19	D16x16	1.986	D16x3	D13-1ctc120	0.528	0.98	B
A 9	400x400	360	3.19	D19x16	2.865	D19x3	D16-1ctc 60	1.655	0.98	B
A 10	400x700	660	1.52	D19x18	1.842	D19x4	D13-1ctc 60	1.056	0.98	B
A 11	500x500	460	2.81	D19x16	1.834	D19x3	D13-1ctc 60	0.845	0.98	B
No.6	400x400	360	3.19	D19x16	2.865	D19x3	D13-1ctc 60	1.056	0.98	B
A 1 (R)	400x400	360	3.19	D19x16	2.865	D19x4	D13-1ctc 80	0.792	0.98	C
A 2 (R)	400x400	360	3.19	D19x16	2.865	D19x4	D13-1ctc 60	1.056	0.98	C
A 3 (R)	400x400	360	3.19	D16x16	1.986	D16x4	D13-1ctc 70	0.905	0.49	B
A 9 (R)	400x400	360	3.19	D19x16	2.865	D19x4	D16-1ctc 60	1.655	0.98	B

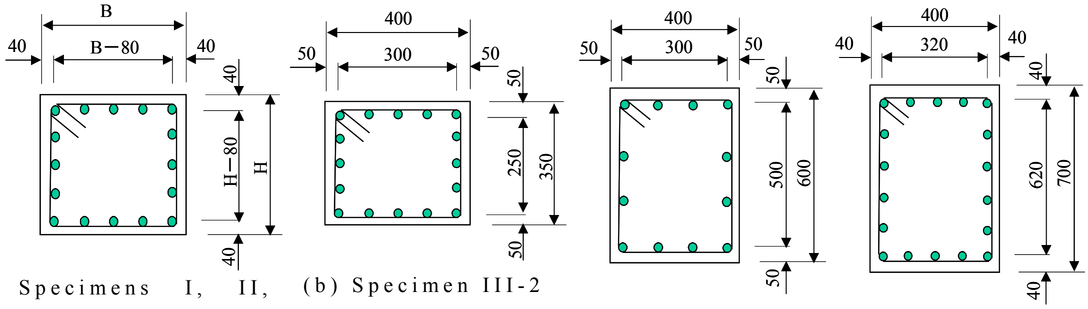

(a) Specimens I, II, III-3,A1~A9,A11,No6 (b) Specimen III-2 (c) Specimen III-1 (d) Specimen A10

Fig. 1 Sectional form of specimens

Table 2 Strength of materials, calculated strength ratio, and test results

Specimen No.	Strength of materials: Compressive strength of concrete (N/mm2)	Strength of materials: Yield strength of axial rein-forcement (N/mm2)	Strength of materials: Yield strength of hoop reinforcement (N/mm2)	Calculated: Vc/Vmu	Calculated: Vs/Vmu	Calculated: Strength ratio Vyd/Vmu	Measured: Ductility factor μ	Measured: Center of rotation h1 (mm)	Measured: Length of damage concentration zone h2 (mm)	Fracture pattern
I - 1	27.4	378.3	359.1	0.66	0.89	1.55	8.9	240	430	Shear after flexural yield
I - 2	23.5	378.3	359.1	0.64	1.62	2.26	11.0	180	360	Bending fracture
I - 3	31.9	378.3	359.1	0.68	2.74	3.42	11.2	140	230	Reinforcement failure
II- 1	28.2	397.2	359.1	0.78	1.68	2.46	10.4	160	360	Bending fracture
II - 2	33.6	397.2	359.1	0.80	2.61	3.40	11.3	100	320	Reinforcement failure
III - 1	32.3	359.1	359.1	1.25	2.66	3.92	24.0	0	130	Reinforcement failure
III - 2	33.7	379.1	359.1	0.69	1.08	1.77	7.3	210	380	Shear after flexural yield
III - 3	32.4	378.3	397.2	0.70	3.48	4.18	10.6	120	280	Reinforcement failure
A 1	26.4	378.4	358.3	0.65	1.39	2.05	10.5	160	360	Bending fracture
A 2	23.3	378.4	358.3	0.64	1.89	2.52	12.4	170	380	Bending fracture
A 3	26.8	397.2	358.3	0.77	2.16	2.94	15.1	140	380	Bending fracture
A 4	28.4	358.3	358.3	1.09	2.78	3.86	20.6	120	290	Bending fracture
A 5	29.1	358.3	358.3	1.08	1.58	2.66	14.8	180	420	Bending fracture
A 6	31.0	378.4	358.3	0.68	2.20	2.87	15.2	140	340	Bending fracture
A 7	30.7	378.4	358.3	0.68	1.83	2.51	12.6	160	340	Bending fracture
A 8	23.8	397.2	358.3	0.75	1.23	1.98	12.1	190	430	Bending fracture
A 9	21.7	378.4	397.2	0.63	3.31	3.94	14.5	120	340	Bending fracture
A 10	22.3	378.4	358.3	0.66	1.35	2.01	11.9	260	550	Bending fracture
A 11	24.6	378.4	358.3	0.66	1.70	2.36	13.7	150	540	Bending fracture
No.6	19.4	375.1	358.3	0.62	1.94	2.56	13.8	150	380	Bending fracture

After carrying out the loading tests, repaired specimens A1, A2, A3 and A9 were designated A1(R), A2(R), A3(R), and A9(R), respectively.

2.2 Loading method

Figure 2 gives an outline of the loading equipment used for static reverse cyclic loading tests under constant axial force. To define the displacement at the point when the outermost axial reinforcement strain reaches the yield strain (obtained through material tests as the yield displacement (dy)), we applied reverse cyclic loading at intervals of 4.9 to 9.8 kN up to 1dy, and at integer multiples of dy at 2dy and beyond.

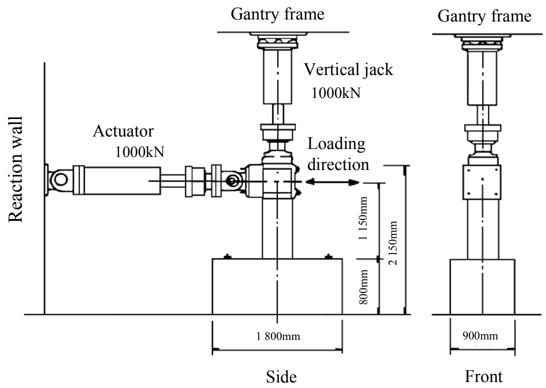

Fig. 2 Loading device

Under loading pattern A in **Table 1**, we applied loads corresponding to the strains at even multiples of dy (2dy, 4dy...) for one cycle after 1dy, and at intervals of 1dy for three cycles after the point where the load dropped. Under loading pattern B, we applied loads at intervals of 1dy at 2dy and beyond.

During reverse cyclic loading tests in the large deformation range, where the ductility factor was 10 or more, some axial reinforcement failed due to low-cycle fatigue under loading pattern A at the initial stage of the study. It should be noted that the possibility of such a fracture pattern is actually very low, since this phenomenon has never been observed in past earthquakes[11]. We also wanted to evaluate the deformation capacity and damage conditions without failure of the reinforcement, and it is for this reason that we selected loading pattern B in place of pattern A for the later tests. Loading pattern C was applied to repaired specimens and consisted of pattern B with the omission of loading at 3dy, 5dy, and 7dy. The maximum loading rate was 120 s per cycle, adjusted to 1 mm/s at the loading point as displacement increased. We continued the tests until the horizontal load fell below about 70% of the yield load.

3. Damage condition after tests

3.1 Fracture pattern and ductility factor

Table 2 shows the test results for ductility factor (dtest/dytest), where dytest is the modified yield displacement from the measurements[8] and dutest is the measured maximum displacement (ultimate displacement) to maintain the yield load (see **Fig. 4**). The measured values in **Table 2** are those for the virgin loading plane. The term "reinforcement fracture" in the fracture pattern column of the table means that the specimen reached the ultimate state after the cover concrete at the base of the loading plane scaled off and part of the axial reinforcement failed. "Shear fracture after flexural yield" means that the specimen reached the ultimate state due to a fracture caused by shear cracking along the line connecting a point between 1.5 and 2.0D in height (D: height of section) and the base of the compressive edge after yielding of the axial reinforcement. "Bending fracture" means that the specimen reached the ultimate state after the axial reinforcement yielded; the cover concrete at the loading plane scaled off from the base to about 1D; and the core concrete gradually pulverized and lost strength.

Figure 3 shows measured values of strength ratio and ductility factor. The strength ratio was set at 2 or more for the specimens used in these tests, except in the case of the two specimens that exhibited shear fracture after flexural yield, so as to give a large deformation capacity at a ductility factor of 10 or more. It is worth noting that the measured value of ductility factor differs according to the loading cycle[8]. When the specimens that underwent bending fracture in these tests are compared after classification by yield stress ratio, however, no major differences in measured value of ductility factor are seen between specimens tested under loading pattern A and those of similar strength ratio and tested under loading pattern B, though the former values are in general slightly smaller than the latter.

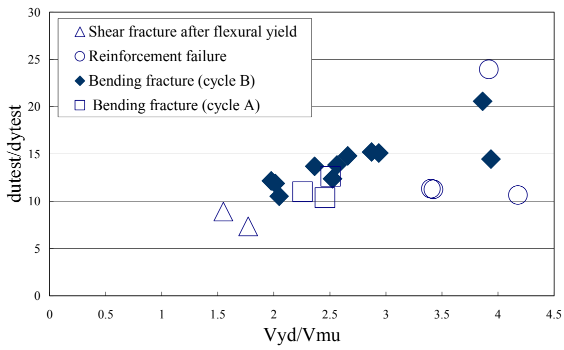

Fig.3 Strength ratio versus ductility factor

3.2 Damage condition

Figure 4 is a schematic illustration of the envelope of the load versus displacement curve of an RC member that underwent shear or bending fracture after flexural yield. In the design to make the plastic deformation level correspond to the damage level, it is conceivable that bifurcation points of the plastic deformation level, A to D, are selected so as to match the damage level in **Fig. 4**. Taking into consideration the effects of parameters within the range tested, damage condition is described below with reference to the model in **Fig. 4**.

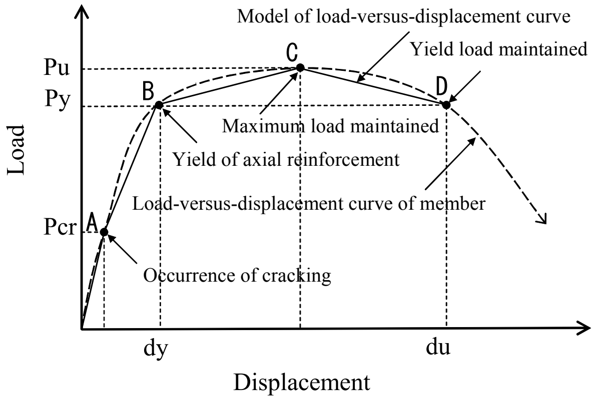

Fig.4 Model of load-versus-displacement curve

a) At yield displacement (point B in **Fig. 4**)

(1) Effect of axial reinforcement ratio

Photos 1 (a) and (b) show the condition of specimens A2 (pa=2.865%) and A5 (pa=1.267%) after 1dy, respectively. These specimens have the same sectional form, the same value of compressive stress intensity, and similar values of strength ratio. **Photo 1 (c)** shows the condition of specimen III-2 (pa=4.424%) after 1dy; this specimen has the largest axial reinforcement ratio of all specimens in these tests, though characteristics other than axial compressive stress intensity are different from the other specimens. The cracking of these specimens is almost the same, aside from minor differences in crack spacing and angle.

(2) Effect of strength ratio (hoop reinforcement ratio)

Photos 1 (d) and (e) show the condition of specimens I-1 (Vyd/Vmu=1.55, ps=0.507%) and I-3 (Vyd/Vmu=3.42, ps=1.584%) after 1dy, respectively. **Photo 1 (f)** shows the test results for specimen III-3 (Vyd/Vmu=4.18, ps=2.274%), which has the highest strength ratio, though its dimensions and axial force are different. Among these specimens, there are no major differences in crack pattern either, though the number of cracks does vary.

(3) Effect of axial force

Photos 1 (g) and (h) show the condition of specimens II-2 (σ'no=1.96N/mm^2) and A3 (σ'no=0.49N/mm^2) after 1dy, respectively. These two specimens along with specimen III-3 (σ'no=4.9N/mm^2) in **Photo 1 (f)**, which has the highest axial force but is otherwise almost the same, there is no great difference in crack pattern.

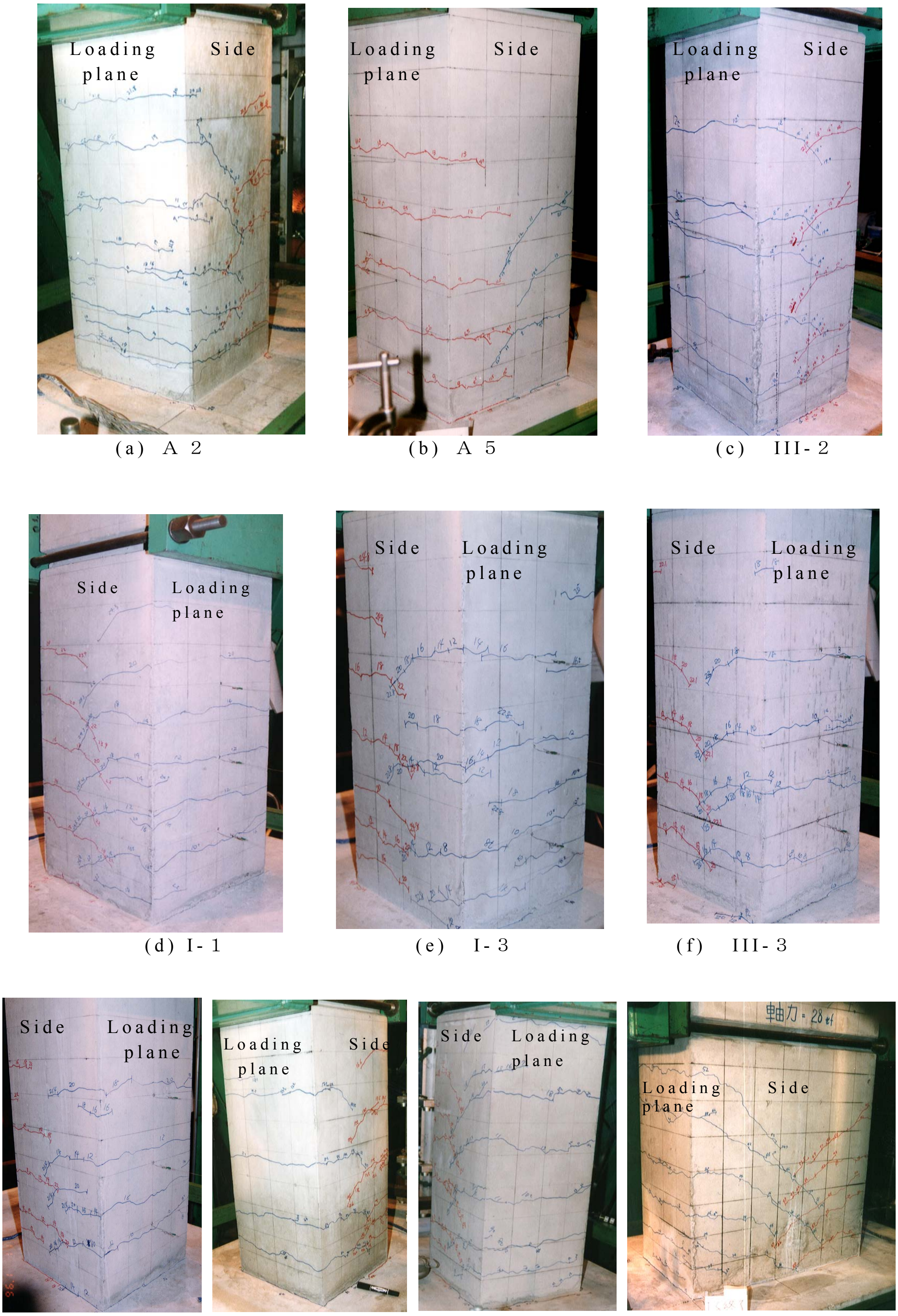

(a) A 2 (b) A 5 (c) III-2

(d) I-1 (e) I-3 (f) III-3

(g) II-2 (h) A 3 (i) A 1 (j) A 10

Photo 1 Damage condition after yield

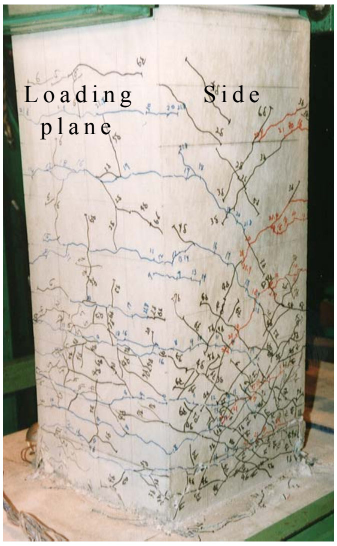

(a) A 2

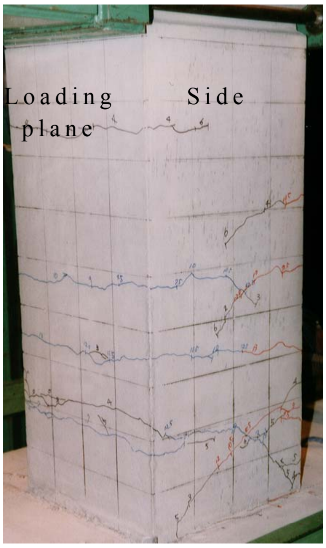

(b) A 5

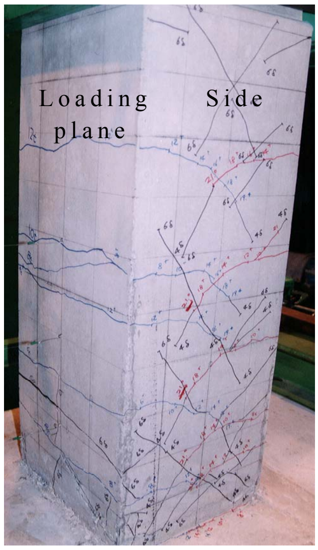

(c) III-2

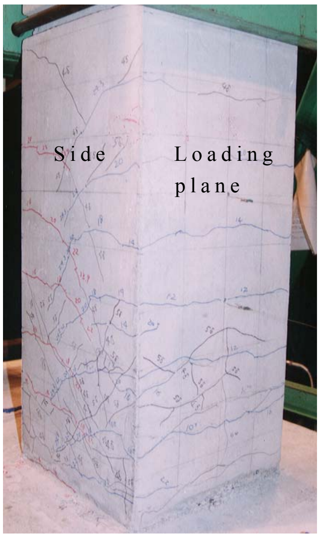

(d) I-1

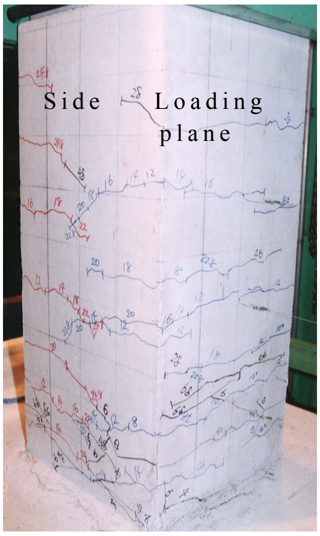

(e) I-3

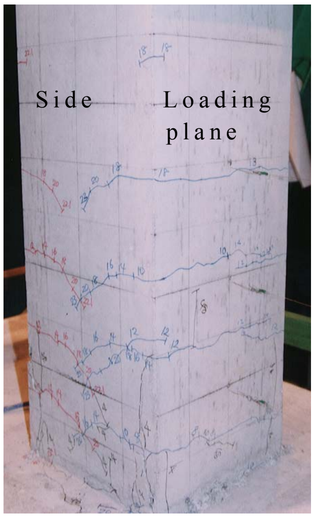

(f) III-3

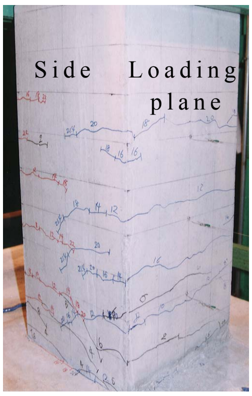

(g) II-2

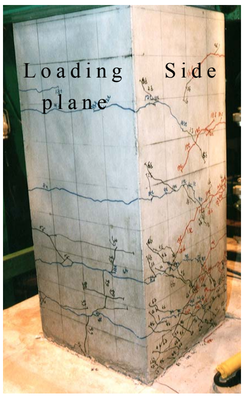

(h) A 3

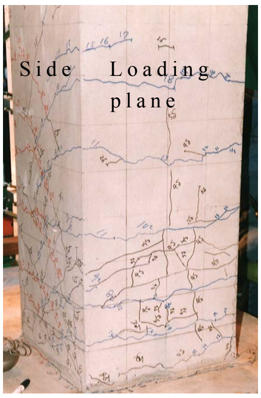

(i) A 1

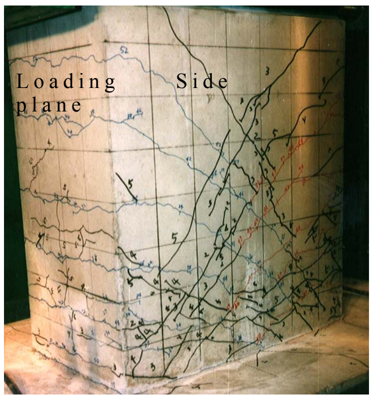

(j) A 1 0

Photo 2 Damage condition after application of maximum

(4) Effect of shear span ratio

Photos 1 (i) and (j) show the test results for specimens A1 (a/d=3.19) and A10 (a/d=1.52), respectively. There are no major differences in cracking between these specimens, which have the same axial compressive stress intensity and similar strength ratio. Since these two specimens underwent bending fracture, a/d seems to have little effect. There are no significant differences either, when the cracking pattern is compared with that of specimen II-3 (a/d=4.17), whose shear span ratio is the largest in the range tested.

As the above discussion demonstrates, there are no major differences in cracking pattern when the specimens yield, though the crack count does vary somewhat. The overall characteristics of the damage condition are summarized below.

Columns suffer bending cracks at a spacing of 150 to 200 mm from the column base up to a position near the loading point before they yield. On the column sides, the tips of bending cracks develop toward the compression zone of the member section, resulting in slanting cracks at 45° to the member axis. However, these cracks do not reach the compression edge. Most of the cracks close when the displacement is returned to 0, suggesting that the residual crack width is extremely small.

b) At maximum load (point C in **Fig. 4**)

(1) Effect of axial reinforcement ratio

Photos 2 (a), (b), and (c) show the condition of specimens A2, A5, and III-2, respectively, after application of the maximum load.

(2) Effect of strength ratio (effect of hoop reinforcement ratio)

Photos 2 (d), (e), and (f) show the test results for specimens I-1, I-3, and III-3, respectively.

(3) Effect of axial force

Photos 2 (g) and (h) show the condition of specimens II-2 and A3, respectively, at the point of maximum loading.

(4) Effect of shear span ratio

Photos 2 (i) and (j) show the test results for specimens A1 and A10, respectively.

Since there are large differences in plastic deformation immediately following application of the maximum load in the case of specimens whose fracture behavior is bending fracture and reinforcement failure (that is, specimens other than I-1 and III-2), large differences are seen in the number and development of cracks. However, there are no significant differences in cracking pattern and crack width when the load is returned to zero. As a general feature of the column sides, shear cracks running from the tension edge at a point about 1D (D: height of section) above the footing toward the antipode side of the loading point at the base reach the compression edge. At the maximum load, the tips of most shear cracks reach the periphery of the compression edge base antipodean to the loading point. The number of bending cracks increases up to a point about 1D above the column base. During load application, the cracks that run from a point about 1D above the footing toward the column base open wider than the other cracks. Above this point, the cracks do not open at all.

In the case of specimens that exhibit shear fracture after flexural yield (I-1 and III-2), the width of the cracks running from above the 1D point toward the column base becomes larger under loading.

The widths of residual cracks when the load is returned to zero after the application of the maximum load are slightly larger irrespective of the fracture pattern. However, the cover concrete does not lift or separate.

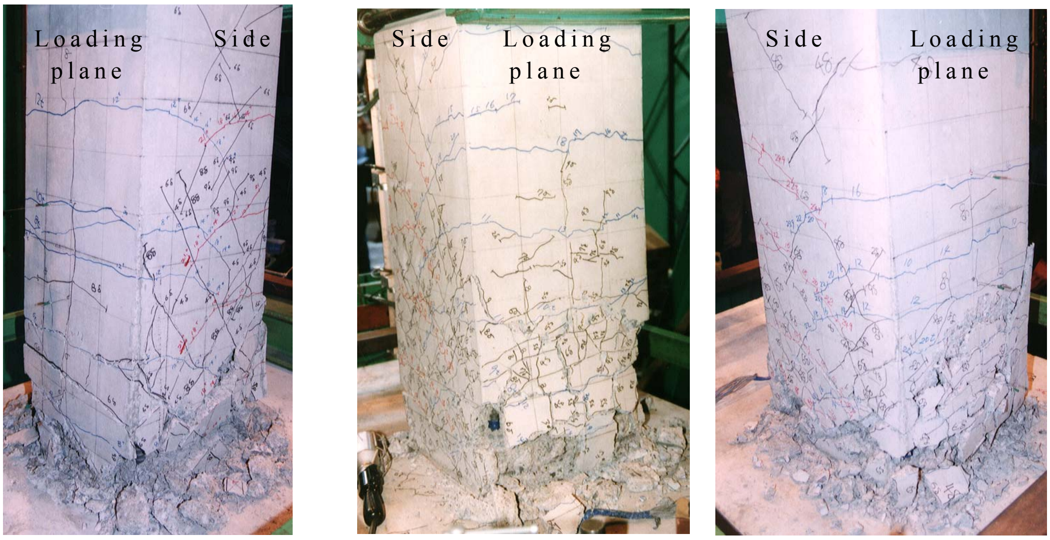

(a) III-2 (b) A 1 (c) I-2

Photo 3 Damage condition at ultimate

c) At ultimate displacement (point D in **Fig. 4**)

The damage to specimens in the ultimate state is summarized below by fracture pattern.

(1) Specimens exhibiting shear fracture after flexural yield

Specimens I-1 and III-3, which exhibit shear fracture after flexural yield, suffer similar damage. As a result of repeated loading after application of the maximum load, the cover concrete on the column sides is seriously damaged and it scales off at the column base. The cover concrete on the loading plane lifts slightly and separates at the base, but the damage is minor when compared with that on the other sides. The strength of the column falls quite rapidly. **Photo 3 (a)** shows specimen III-2 after the ultimate state is reached.

(2) Specimens exhibiting bending fracture

Within the range of these tests, there are no significant variations in damage for different parameter values. For all specimens that exhibit bending fracture, dominant shear cracks occur along the line connecting the column base compression edge with the tension edge about 1D above the footing. While deformation repeats thereafter with the intersection of shear cracks generated by reverse cyclic loading as the center of rotation, the cover concrete in the orientation of the loading plane separates and the axial reinforcement starts to swell. No sharp decrease in strength occurs despite the progression of damage. However, the specimen does lose strength as core concrete subject to compression around the 1D zone (where damage is concentrated) is gradually pulverized into granules by repeated loading.

As mentioned above, the measured values of ductility factor are slightly different for loading patterns A and B. However, the damage is little different at or before the ultimate state in the range of loading tested. **Photos 3 (b) and (c)** show the damage to specimens A1 and I-2 after the ultimate state is reached. The parameters of these specimens are almost identical aside from the loading pattern they experience.

Figure 5 is a schematic representation of the observed damage within a specimen that underwent bending fracture. The separated and pulverized concrete was removed after the loading test to enable visual observations to be made. In the zone where damage is concentrated, the internal concrete has been completely loosened by shear cracks connecting the column base compression edge with a point about 1D above the footing. The concrete sandwiched between these shear cracks (the hatched area in **Fig. 5**) is damaged and pulverized into wedge-shaped forms.

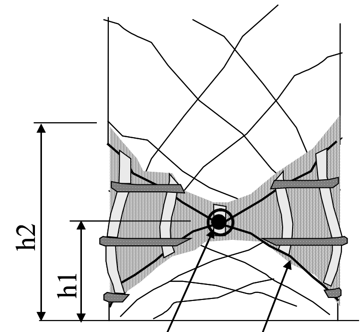

Fig. 5 Conceptual drawing of damage condition after scaling-off of cover concrete

4. Discussion of damage

4.1 Discussion of damage level (ease of repair)

We first discuss the damage level (which corresponds to ease of repair) with respect to the plastic deformation levels shown in **Fig. 4** based on the test results. Since, in order to prevent collapse of the structure, the design of the columns precludes shear fracture even after flexural yield, the discussion focuses on the test results for specimens that suffered bending fracture. As mentioned in the previous section, there is virtually no difference in damage for different parameter values within the range of these tests. However, evaluation of the dimensionless plastic deformation levels, as discussed later, requires proper determination of the ductility factor. In discussing the effect of loading cycles, therefore, we will compare results with different parameter values.

In cases where shear cracking does not take place first, the occurrence of such cracking constitutes a bifurcation point determining whether or not use of the structure can continue without repair after an earthquake. As mentioned in the previous section, if the column section is undamaged and the residual crack width is small at yield or at the maximum load, then it is assumed that the column may continue in use without repair.

Next, we discuss whether grouting is an adequate method of crack repair, or whether it is possible to set the bifurcation point of damage level depending on the necessity of repair in order to repair the column section. Since the section must be repaired if large areas of cover concrete have lifted or scaled off, a quantitative evaluation of damage at the plastic deformation level was carried out. In this context, visual observation is used to judge whether the amount of cover concrete that has lifted or separated is "large". Strictly speaking, the concrete will have partially lifted prior to that point. In the past, however, columns have been restored to the proper section after earthquake damage simply by resin grouting, unless the lifted area of concrete was observed to be "large"12),13). Based on this experience, we chose to carry out repairs by grouting only for columns that do not exhibit large areas of lifted or separated cover concrete.

Figure 6 shows the relation between strength ratio and the ratio du'/dutest, which is the maximum displacement at the loading point during the loading loop in which the cover concrete on the loading plane scaled off (du') to the ultimate displacement (dutest). There is no identifiable correlation between strength ratio and du'/dutest. In the case of specimens that suffer bending fracture, the concrete on the loading plane separates at 80%

to 90% of the ultimate displacement (dtest), and differences in loading pattern do not affect this. In the case of specimens that suffer shear fracture after flexural yield or reinforcement failure, the concrete on the loading plane scales off at displacements greater than 80% to 90% of the ultimate displacement (dtest). Since the ultimate displacement is seen to increase when specimens that suffer reinforcement failure undergo bending fracture without failure due to low-cycle fatigue, the concrete will scale off at displacement ratios smaller than shown in **Fig. 4** in the case of concrete columns with dimensions equivalent to those of the four specimens that suffered reinforcement failure in this study.

Figure 7 shows the relation between strength ratio and du''/dutest, which is the ratio of maximum displacement at the loading point in the range where the damage on the section is limited at the cover concrete surface layer at the base of loading plane (du'') to the ultimate displacement (dutest). In the case of specimens that suffer bending fracture, the surface layer of the cover concrete at the loading plane base suffers slight damage up to a displacement equivalent to 60% to 80% of the ultimate displacement (dutest), and this is not affected by the number of loading cycles. It is thought that columns with damage no worse than this can continue in use after grouting the cracks. As shown in **Fig. 8**, the ratio (P1/Putest), which is the ratio of strength (P1) on the loading loop to maximum load (Putest), is little affected by the number of loading cycles in the case of specimens that suffer bending fracture. This ratio is 97.2% on average, meaning that P1 is almost the same as Putest.

Figure 9 shows the relation between strength ratio and du'''/dutest, the ratio of displacement at maximum load (d''') to ultimate displacement (dutest). In this study, the point where the measured horizontal working force is the largest is taken as the point where the maximum load is applied. Since the load envelope has an extremely gentle gradient around point (C) where the maximum load is applied, the value is ambiguous and du'''/dutest has considerable scatter. In the case of specimens that suffer bending fracture, however, the displacement at the point where the maximum load is applied (point C) is less than 60% of the ultimate displacement, despite variation in the number of loading

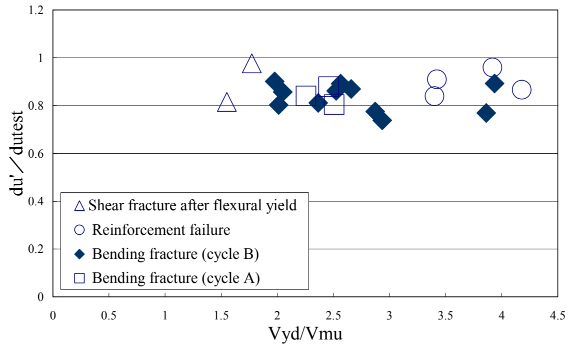

Fig. 6 d'/dutest versus strength ratio

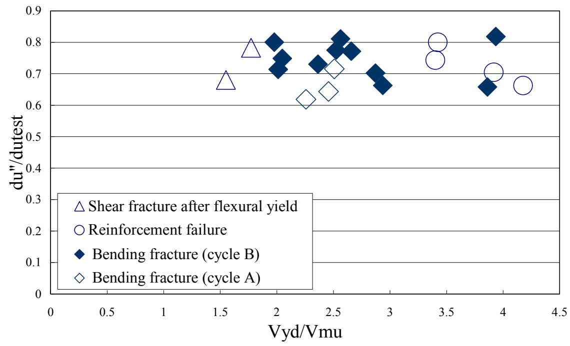

Fig. 7 d''/dutest versus strength ratio

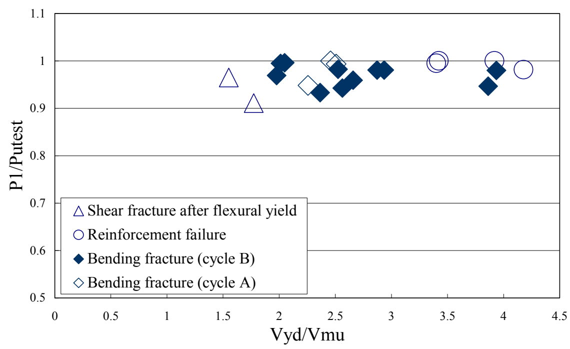

Fig. 8 P1/Putest versus strength ratio

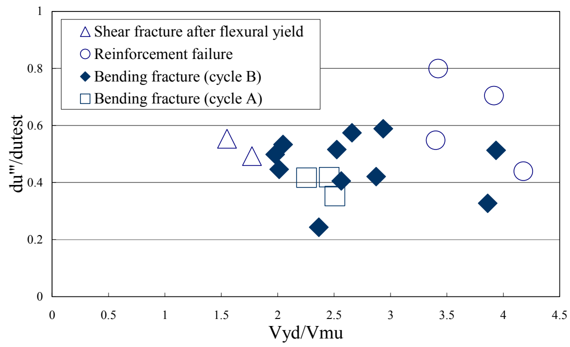

Fig. 9 du'''/dutest versus strength ratio

cycles. In taking the point of maximum measured horizontal working force as the point of maximum load, as in this study, the expectation is that no scaling of concrete will occur even after the maximum load, and columns are repairable by grouting only in the range where a constant strength is maintained, or from the point where the maximum load is applied to the point where the cover concrete lifts to a large extent or separates.

In this study, we also compared the horizontal displacement at maximum horizontal load and zero horizontal load with the load when the horizontal displacement is zero.

Figure 10 shows the displacement (drpu) at the zero load point during the loading loop at maximum load, as well as the relation between strength ratio and di/dutest (di=drpu or dru), the ratio of residual displacement at zero load during the loading loop at the ultimate state (dru) to the ultimate displacement (dutest). **Table 3** gives values of these variables for each specimen. In the case of specimens that underwent bending fracture, the zero-load displacement in the ultimate state is about twice that at the maximum load, irrespective of loading cycle. **Figure 11** shows the relation between strength ratio and the ratio (Pi/Putest) of the load required to return the displacement at zero load to the neutral position (Pi) to the maximum load (Putest), where Pi is Prpu or Pru (Prpu: load required to return the displacement at zero load during the loading loop at the maximum load to the neutral point) and Pru is the load required to return the displacement at zero load during the loading loop at the ultimate state to the neutral point. **Table 3** also gives values of these variables for each specimen. In the case of specimens that suffered bending fracture, Prpu/Putest and Pru/Putest are about 0.5 and 0.4, respectively, irrespective of loading cycle. From this result, it can be said that the displacement at zero load in the ultimate state is about twice that at the maximum load, and the load required to return the displacement to the neutral point is almost the same in these two states on the load-versus-displacement hysteresis route in static loading tests.

Figure 12 summarizes the symbols used in the above discussion.

Table3 di/dustst and Pi/Putest

	drpu /dutest	dru /dutest	Prpu /Putest	Pru /Putest
I - 1	0.31	0.52	0.55	0.33
III - 2	0.30	0.86	0.54	0.21
I - 3	0.56	0.59	0.60	0.54
II - 2	0.37	0.80	0.49	0.36
III - 1	0.32	0.71	0.39	0.21
III - 3	0.29	0.78	0.84	0.77
I - 2	0.24	0.56	0.55	0.43
II - 1	0.26	0.62	0.45	0.34
A 7	0.20	0.73	0.46	0.28
A 1	0.35	0.71	0.49	0.44
A 2	0.34	0.72	0.55	0.44
A 3	0.44	0.72	0.59	0.43
A 4	0.22	0.84	0.47	0.35
A 5	0.41	0.77	0.48	0.45
A 6	0.26	0.78	0.50	0.37
A 8	0.39	0.65	0.50	0.46
A 9	0.33	0.75	0.53	0.38
A10	0.22	0.73	0.43	0.15
A11	0.10	0.62	0.28	0.41
No6	0.26	0.73	0.51	0.48

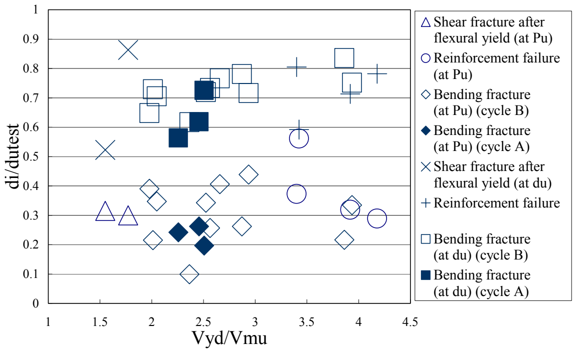

Fig. 10 di/dutest versus strength ratio

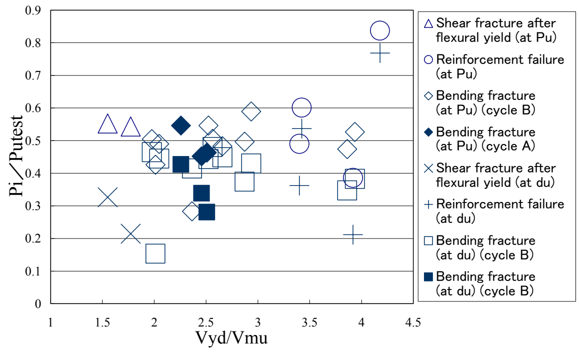

Fig. 11 Pi/Outest versus strength ratio

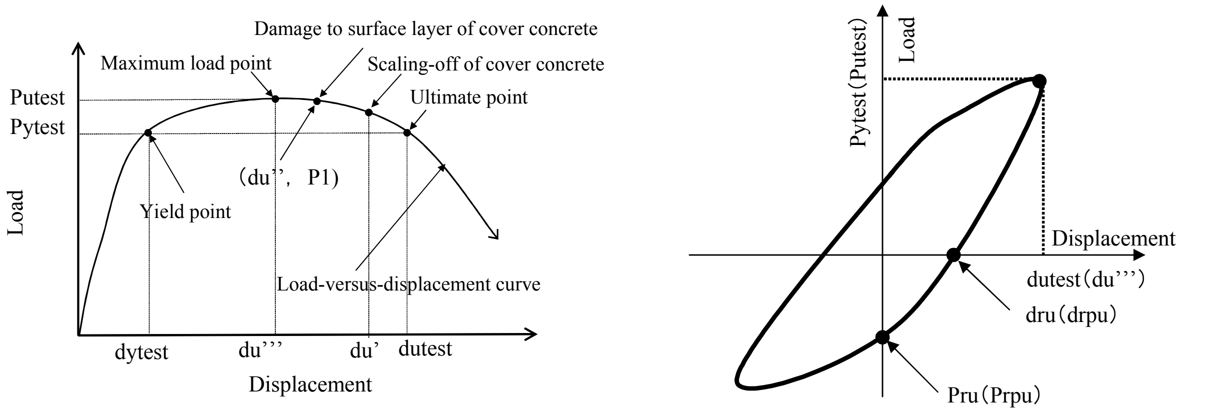

(a) du',du'',du''',dutest,P1,Pytest,Putest (b) dru and Pru (in the ultimate state) and drpu and Prpu (at the maximum load)

Fig. 12 Explanation of symbols

4.2 Discussion of damage concentration zone

a) Center of rotation and height of damage concentration zone

Figures 13 and 14 show the length (h2) of the damage concentration zone, as schematically illustrated in **Fig. 5**, and the relation between strength ratio and the ratio of height (h1) of the intersection point between dominant shear cracks (center of rotation) to the height (D) of section.

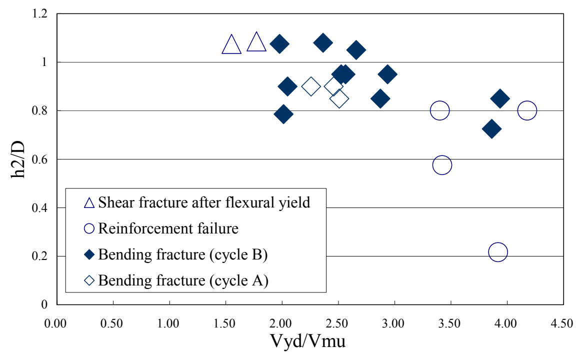

Fig.13 h2/D versus strength ratio

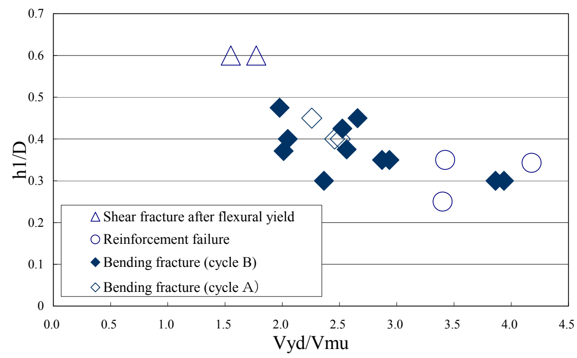

Fig. 14 h1/D versus strength ratio

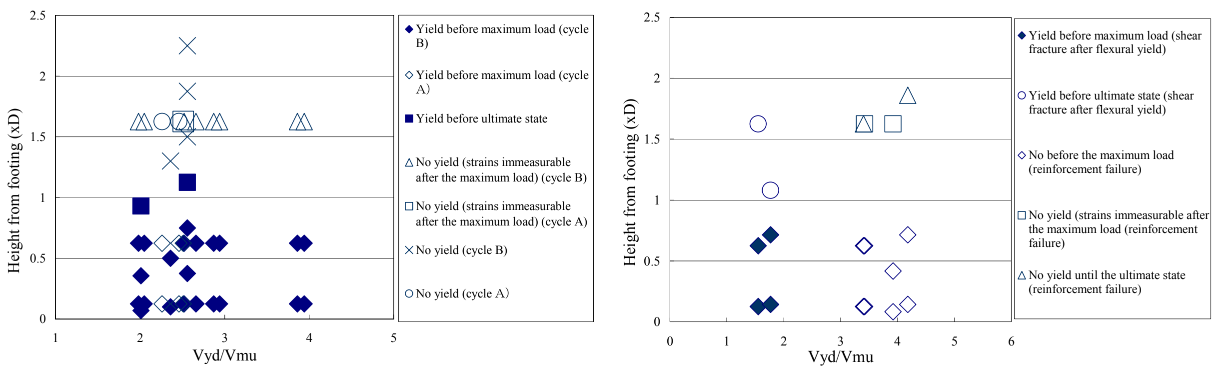

(a) bending fracture (b) shear fracture

Fig.15 Yield range of axial reinforcement

In the case of specimens that underwent bending fracture, loading cycle has little effect. There is a negative correlation between strength ratio and h2/D and h1/D. The position of the center of rotation, h1, which is about 0.45D for a strength ratio of 2, tends to fall slightly as the strength ratio increases.

b) Yield range of axial reinforcement

Figures 15 (a) and (b) show results of using strain measurements to judge whether the outermost axial reinforcement has yielded for those specimens that underwent bending fracture and those that underwent shear fracture and reinforcement failure after flexural yield, respectively.

Since the strain was measured only at the points shown in the Figure. it is not possible to determine the yield range of the main reinforcement based on these figures. However, a number of general trends can be observed.

The yield position of specimens that underwent shear fracture after flexural yield was 1D or more above the column base, and yielding took place after application of the maximum load and before the ultimate state was reached. This is an inevitable outcome since the dominant cracks occurred along a slanting line connecting the column base and points above the 1D point.

In the case of specimens that underwent bending fracture, most strains increased beyond the capacity of the strain gauges before the ultimate state, so it is impossible to judge the ultimate behavior of the reinforcement. In the range of our tests, however, the outermost reinforcement yielded up to about the 1D point, but possibly not above the 1.25D point.

5. Confirmation of repair effectiveness

5.1 Method of repair and outline of tests

Table 1 summarizes the dimensions of the specimens. We repaired specimens A1, A2, A3, and A9 after the reverse cyclic loading tests and denoted the repaired specimens A1 (R), A2 (R), A3 (R), and A9 (R), respectively. Repairs were carried out using the materials shown in **Table 4** in the order shown in **Table 5**. **Table 6** gives the strength of

Table 4 Materials used for repair

No	Materials	
	Crack grouting	Repair of section
A 1(R)	Epoxy resin	Epoxy resin mortar
A 2(R)	Acrylic resin	Ultra rapid hardening cement and some polymer cement
A 3(R)	Cement-based ultra-fine particle crack grouting material	Polymer cement mortar
A 9(R)	——————	Premix mortar

Table 5 Order of work

Order	Work
1	Cleaning of specimen after reverse cyclic loading tests
2	Check of cracks in column member
3	Installation of crack grouting jig
4	Assembling of section repairing formwork
5	Kneading, mixing, casting, and curing of section repairing material
6	Removal of formwork
7	Application of seal to prevent flowage of crack grouting material
8	Kneading, mixing, casting, and curing of crack grouting material
9	Removal of jig and seal

the various repair materials. Any pulverized concrete was removed and where axial reinforcement and hoop reinforcement had swelled or deformed it was replaced. Since the axial reinforcement in specimens A2 (R), A3 (R), and A9 (R) had swelled considerably, it was not possible to restore them to their original sectional form (400 x 400 mm); in these cases the section was increased to 440 mm (loading plane) x 470 mm

Table 6 Strength of repair materials

Test item	Unit	Crack repairing material			Section repairing material			
		Epoxy resin	Acrylic resin	Cement-based ultra-fine particle crack grouting material	Epoxy resin mortar	Ultra rapid hardening cement mortar	Polymer cement mortar	Premix mortar
Viscosity	cps	560		500				
Specific gravity		1.22	1.18		1.6			
Compressive strength	N/mm^2	66.7		20.4~ 24.5	47.5	46.0	35.7~ 40.8	56.8
Bending strength	N/mm^2	56.8	66.5		19.4			
Tensile strength	N/mm^2	37.4						4.0

(other two sides) up to 300 mm from the top of the footing for specimen A2 (R); 440 mm x 440 mm up to 315 mm from the footing top for A3 (R); and 415 mm x 470 mm up to 450 mm from the footing top for A9 (R).

Since the axial reinforcement had already yielded, we applied loads corresponding to displacements that were integer multiples of the measured yield displacement (dy) before repair.

5.2 Test results and discussion

a) Damage

The repaired specimens all suffered similar damage. The damage to specimen A2 (R) is described below.

Photo 4 (a) shows the state of A2 (R) after 1dy (where dy is the measured displacement of specimen A2). Only minor cracking of the repaired area took place after 1dy, presumably because the strength of the repair material was higher than that of the original concrete. **Photo 4 (b)** shows the state immediately after application of the maximum load, when wide dominant cracks were seen along the slanting line connecting the column base and points about 1D above the footing. This is similar to the damage to specimen A before the repair (in the "virgin loading test"). **Photo 4 (c)** shows the condition of the specimen in the ultimate state. After application of the maximum load, deformation repeated around the intersection point between shear cracks that connect the column base and points about 1D above the footing (the center of rotation). This caused the concrete sandwiched by cracks to be pulverized (the hatched part in **Fig. 5**), and the column gradually lost strength until it reached the ultimate state with a bending fracture pattern. Specimens other than A2 (R) reached the ultimate state after the maximum strength due to failure of the axial reinforcement caused by low cycle fatigue.

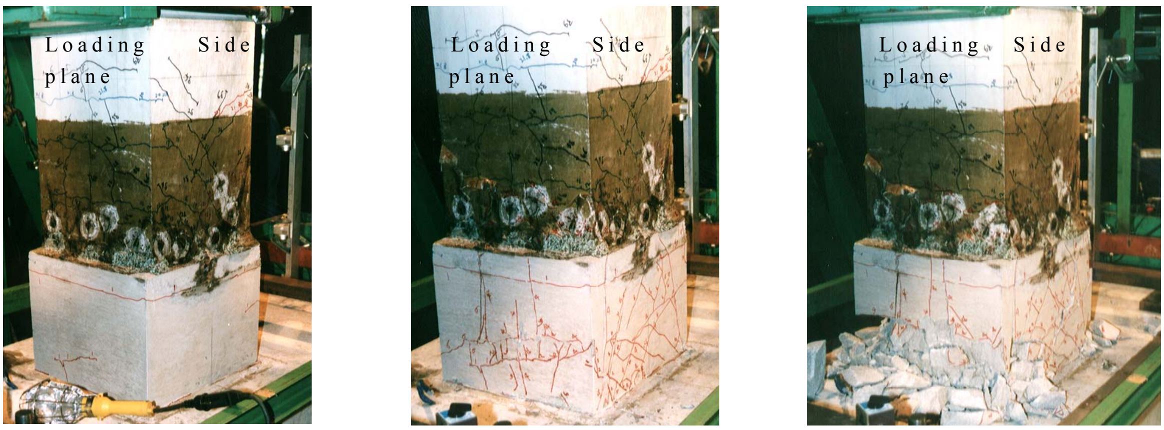

(a) After yield (b) After the maximum load (c) After the ultimate state

Photo 4 Damage condition of repaired specimen

b) Deformation capacity

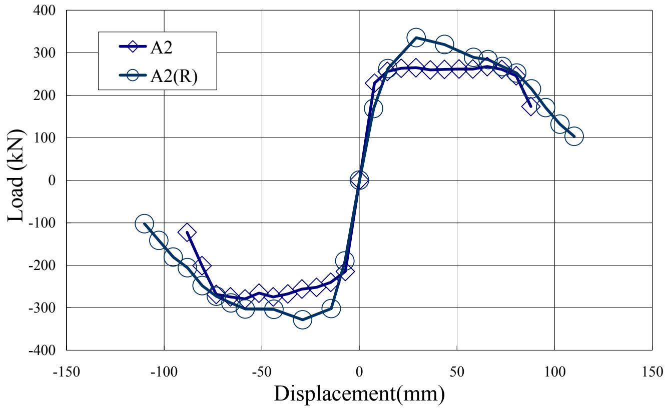

fig.16 Envelopes of the load versus displacement curves of A2 and A2(R)

Figure 16 compares the envelopes of the load-versus-displacement curves for specimens A2 and A2 (R), in which the axial reinforcement did not fail. Other specimens that reached the ultimate state as a result of reinforcement failure behaved similarly to A2 (R), except that strength fell somewhat sharply as a result of reinforcement failure after application of the maximum load. In other words, for all repaired specimens except A4 (R) (which was repaired with premix mortar), the maximum load was higher after repair since the base cross section was greater, even though the initial rigidity was slightly lower than in the virgin loading test. **Table 7** summarizes the test results, with the ratios of initial rigidity, maximum load, equivalent viscous damping constant, and energy absorption being the ratio to corresponding variables measured in the virgin loading tests. In calculating the ductility factor after repair, we took the maximum displacement to maintain the yield load in the virgin loading test as the ultimate displacement after repair, and the modified measured value (dytest 5)) of yield displacement in the virgin loading tests (corrected by the ratio of initial loss in rigidity) as the yield displacement after repair. We took the secant rigidity at the yield point (the point corresponding to the yield displacement in the virgin loading tests for repaired specimens) as the initial rigidity. The ratio of equivalent viscous damping constant is the value, averaged over all loading loops, of the ratio of values in the virgin loading tests to those in the repaired specimen tests at integer multiples of dy. The ductility factors of members after repair, calculated according to the above definition, are slightly lower than those in the virgin loading tests. However, values of about 10 are obtained as long as the reinforcement does not fail, as shown in **Table 7**.

Table 7 Test results of repaired specimens

	Initial rigidity ratio	Maximum load ratio	Ductility factor	Equivalent viscous damping constant ratio	Energy absorption ratio	Fracture pattern
A 1	1.00	1.00	10.50	1.00	1.00	Bending fracture
A 1 (R)	0.77	1.19	13.40	0.90	2.83	Reinforcement failure
A 2	1.00	1.00	12.40	1.00	1.00	Bending fracture
A 2 (R)	0.78	1.27	10.10	0.77	1.20	Bending fracture
A 3	1.00	1.00	15.10	1.00	1.00	Bending fracture
A 3 (R)	0.91	1.19	9.60	0.75	0.86	Reinforcement failure
A 9	1.00	1.00	14.50	1.00	1.00	Bending fracture
A 9 (R)	0.67	1.08	8.90	0.65	0.98	Reinforcement failure

The equivalent viscous damping constant decreased with each cycle after repair from the value obtained in the virgin loading tests. This is particularly notable in the case of specimen A9 (R), whose section was repaired using premix mortar without crack grouting. Although the equivalent viscous damping factor fell slightly, however, the energy absorbed up to the ultimate state was greater than in the virgin loading tests in cases where the reinforcement did not fail. It has been reported that, in practice, reinforcement rarely fails due to low cycle fatigue caused by repeated earthquake motion11). It is thought, therefore, that even RC columns subjected to large deformation at a ductility factor of about 10 may have an earthquake resistant capacity equivalent to that before repair, as long as the section is repaired and cracks are filled with a grouting material.

6. CONCLUSION

6.1 Damage condition

The following conclusions can be drawn from the experimental results and discussions presented here:

a) Bending and shear cracks appear near the loading point before yield. Most of these cracks close when the displacement is returned to zero, suggesting that the residual crack widths are extremely small. Therefore, continued use is possible without repair in the case of loads like this.

b)Once the maximum load is reached, the residual cracks are slightly wider when the load is returned to zero, irrespective of the fracture pattern. However, the cover concrete does not lift or separate. In this case, repairs to the column section by resin grouting are sufficient to restore the earthquake damage. Furthermore, in cases where bending fracture occurs, displacement under the maximum load is less than 60% of the ultimate displacement irrespective of differences in the number of loading cycles.

c) In the case of bending fracture, the cover concrete surface layer at the loading plane base is slightly damaged up to a displacement equivalent to 60% to 80% of the ultimate displacement. It is thought that columns can continue in use after grouting the cracks if the damage is no worse than this. The ratio P1/Putest of strength ratio at the loading loop (P1) to the maximum load (Putest) is little affected by the number of loading cycles where bending fracture occurs. The ratio P1/Putest is 97.2% on average, meaning that P1 is almost the same as Putest.

d) Where bending fracture occurs, the concrete of the loading plane separates at 80% to 90% of the ultimate displacement (dtest). After such damage, the section needs to be repaired.

e) Where bending fracture occurs, the ultimate state is reached after yielding of the axial reinforcement, the cover concrete at the loading plane scales off between the base and a height of about 1D, and the core concrete is gradually pulverized and thus loses strength. Repairs to the column section are necessary.

f) From the above, it can be said that the displacement at zero load in the ultimate state is about twice that at the maximum load and the loads required to return the displacement to zero are almost the same in these two states on the load-versus-displacement hysteresis curve in static loading tests.

g) Where bending fracture occurs, there are negative correlations between strength ratio and both h2/D and h1/D. The center of rotation, h1, which is about 0.45D for a strength ratio of around 2, tends to move downward slightly as the strength ratio increases.

h) Where shear fracture occurs after flexural yield, the yield point is 1D or more above the column base after application of the maximum load and before the ultimate state is reached. In test range studied, the outermost reinforcement yielded up to about 1.5D above the base. Where bending fracture occurred in the tests, most strains increased beyond the capacity of the strain gauges before the ultimate state, making it impossible to judge the ultimate behavior of the reinforcement. In the test range studied, however, the outermost reinforcement yielded up to about 1D above the base, but probably not beyond 1.25D.

6.2 Deformation capacity of repaired specimens

a) The ductility factor of members after repair calculated according to the our definition is slightly lower than that in the virgin loading tests. However, values of about 10 can be obtained as long as the reinforcement does not fail.

b) The equivalent viscous damping constant decreases in each cycle after repair from the value obtained in virgin loading tests. This decrease was particularly prominent in a specimen whose section was repaired using premix mortar without crack grouting. Although the equivalent viscous damping factor falls slightly with increasing number of cycles, the energy absorbed up to the ultimate state is greater than in the virgin loading tests, as long as the reinforcement does not fail.

c) It is thought, therefore, that even RC columns subjected to large deformation at a ductility factor of about 10 may have an earthquake resistant capacity equivalent to that before repair if the section is fully repaired and cracks are filled with a grouting material.

References

[1] Railway Technical Research Institute, Standard specification for design of concrete structure for railways, 1992 (in Japanese)

[2] Japan Society of Civil Engineers, Standard Specifications for Concrete Structures (seismic design), 2002

[3] Railway Technical Research Institute, Standard specification for seismic design of structures for railways, 1999 (in Japanese)

[4] Tsuyoshi, T., Kobayashi, M., and Ishibashi, T., “Damage of RC Columns Subjected to Reversal Cyclic Loading”, Proc. of JCI, Vol.21, No.3, pp.1171-1176, 1999 (in Japanese)

[5] Umihara, T., Kobayashi, K., and Ishibashi, T., “A Study on the Repair Effect of Damaged RC Columns that Subjected to Reversal Cyclic Loading”, Symposium regarding 'The Seismic Resistance Reinforcement, Technology of Repairing, Technology of Diagnosis', JSCE, 1998 (in Japanese)

[6] Niwa, J., Yamada, K., Yokozawa, k., and Okamura, H., “Revaluation of the Equation for Shear Strength of Reinforced Concrete Beams without Web Reinforcement”, Proc. of JSCE, No.372/V-5, pp.167-176, 1986 (in Japanese)

[7] Ishibashi, T.,Matsuda, Y., and Saito, K., “Proposed Design Method of the Shear Strength of Reinforced Concrete Footings with a Few Piles”, Proc. of JSCE, No.337, pp.197-204, 1983 (in Japanese)

[8] Umihara, T., Kobayashi, K., and Ishibashi, T., “Study on Estimation of the Yield Displacement under Earthquake on RC Columns”, Proc. of JCI, Vol.21, No.3, pp.1213-1218, 1999 (in Japanese)

[9] Machida, A., Matsuyoshi, H., and Toyoda, K., “Evaluation of the Ductility of Reinforced Concrete Members”, Proc. of JSCE, No.378/V-6, pp.203-212, 1987 (in Japanese)

[10] Shima, H., Chou, L., and Okamura, H., “Bond-Slip-Strain Relationship of Deformed Bars Embedded in Massive Concrete”, Proc. of JSCE, No.378/V-6, pp.165-174, 1987 (in Japanese)

[11] Japan Concrete Institute, Symposium Committee Report Regarding that the Situation of the Deterioration of Plasticity Area that by Cyclic Loading, pp108, 1998 (in Japanese)

[12] Japanese National Railroad, SENKANKO ’1978, Feature issue on

"Earthquake off the Coast of Miyagi Pref.", pp15-46, 1979 (in Japanese)
[13] East Japan Railway Company, The Report of Hanshin-Awaji Earthquake Disaster and Railways 〔1st volume / Damage and Reconstruction〕, pp229-235, 1996 (in Japanese)